

## Assessment of tropospheric modeling on PPP-AR performances under brazilian atmospheric condition

Lais Thuany Cardoso Theodoro<sup>1</sup> - ORCID: 0000-0001-6232-122X

Tiago Lima Rodrigues<sup>2</sup> - ORCID: 0000-0002-3037-9037

Paulo Sérgio de Oliveira Junior<sup>2</sup> - ORCID: 0000-0001-7000-6924

Kauê de Moraes Vestena<sup>1</sup> - ORCID: 0000-0003-1225-2371

<sup>1</sup>Universidade Federal do Paraná, Setor de Ciências da Terra, Departamento de Geomática, Programa de Pós-Graduação em Ciências Geodésicas, Curitiba - Paraná, Brasil.

E-mails: laistheodoro@ufpr.br; kauemv2@gmail.com

<sup>2</sup>Universidade Federal do Paraná, Setor de Ciências da Terra, Departamento de Geomática, Curitiba - Paraná, Brasil.

E-mails: tiagorodrigues@ufpr.br; paulo.junior@ufpr.br

Received in 30<sup>th</sup> May 2020.

Accepted in 1<sup>st</sup> June 2022.

### Abstract:

In the Global Navigation Satellite System (GNSS), ambiguity resolution (AR) can shorten observation time and increase the positioning quality. The correct tropospheric modeling is intrinsically related to the ability to perform AR. Here, we assessed the influence of different tropospheric correction alternatives on AR for static Precise Point Positioning (PPP) in Brazilian territory. Our goal was to provide directions to users when choosing a suitable tropospheric model for application in PPP-AR under Brazilian atmospheric conditions. Thus, this study was carried out using well-known models such as the Saastamoinen model and the Zenith Tropospheric Delay (ZTD) Estimation and Numerical Weather Prediction (NWP) model from CPTEC/INPE. Six GNSS stations from the Brazilian Network for Continuous Monitoring (RBMC) (BRAZ, UFPR, RNNA, POVE, SMAR, and SAGA) were selected. Different GNSS processing setups were considered for GNSS data registered at selected stations during summer and winter. The assessment was based on a statistical analysis of positioning accuracy during one-hour sessions. The results indicated that such as the ZTD Estimation, the NWP model provides an accuracy of a few centimeters. On the other hand, the Saastamoinen model provided decimeter level accuracy, thus it is not the recommended choice for PPP-AR in the experimental conditions.

**Keywords:** Precise Point Positioning; Tropospheric modeling; Ambiguity resolution; Numerical Weather Prediction Model.

**How to cite this article:** Theodoro LTC, Rodrigues TL, Oliveira Junio PS, Vestena KM. Assessment of tropospheric modeling on ppp-ar performances under brazilian atmospheric condition. *Bulletin of Geodetic Sciences*. 28(3): e2022013, 2022.



This content is licensed under a Creative Commons Attribution 4.0 International License.

## 1. Introduction

Over time, different data processing techniques have emerged that use the Global Navigation Satellite System (GNSS). Among these, Precise Point Positioning (PPP) has been extensively investigated by the scientific community. This is due to the availability of free software and online services that enable this processing method. Unlike the relative and differential positioning, in general, the conventional PPP solution does not depend on data sources from other stations (Ge et al. 2008). Besides, it is the most indicated method for geodynamic, environmental, and meteorological studies, among others (Zhang et al. 2017; Zheng et al. 2019).

The PPP applications are diverse and go much further providing instantaneous position and velocity of a point (Ge et al. 2008; Li, Li and Gao, 2015). As examples, one could mention studies of earth crust deformation monitoring (Zheng et al. 2019), GNSS-meteorology (Shi et al. 2015; Zhang et al. 2017), velocity field determination (Perez, Monico and Chaves, 2003), precision agriculture (dos Santos et al. 2017), up to the determination of satellite orbits (Yoshioka and Murata 2009; Choi et al. 2012). In this scenario, the scientific community seeks ways to guarantee greater accuracy for this positioning method. Examples of early researches include Zumberge et al. (1997) and Kouba and Héroux (2000). PPP has advanced much further after the pioneering researches of these authors. Examples of the latest researches include Teunissen and Khodabandeh (2015) and Pan et al. (2021).

Traditionally, in the PPP process, the carrier phase ambiguity resolution (AR) is not considered, e.g., no attempt is made to estimate integer ambiguity values. In recent years, research has been conducted to investigate the AR issue in PPP, as well as its influence on the quality of positioning and the field observation time. As examples of the research that investigates the AR issue in PPP, we can mention Teunissen, Odijk, and Zhang (2010) who describe PPP-RTK ambiguity resolution. Laurichesse (2011) presents the architecture of a complete real-time 'integer PPP' demonstrator developed by CNES; it also presents results obtained within the framework of the Real-Time IGS Pilot project, as well as results from a stand-alone experiment. Shi and Gao (2014) compare three PPP integer ambiguity resolution methods, the decoupled clock model, which includes the single-difference between-satellites model, and the integer phase clock model. Li, Li, and Gao (2015) approach the stochastic modeling of atmospheric corrections and analyze their effects on the PPP AR efficiency. Geng and Shi (2017) propose a composite strategy, where simultaneous GPS and GLONASS dual-frequency PPP-AR is carried out, to improve the reliability of partial AR.

In Brazil, Alves, Monico and Romão (2011) evaluate the resolution of ambiguities in PPP at different observation times. Lima, Monico and Marques (2016) investigates and adopts a methodology for PPP integer ambiguity resolution based on a GNSS network. To reduce the time to achieve accurate positions, de Oliveira et al. (2017) modeled the behavior of the troposphere over France using tropospheric delay estimates at Orpheon GNSS reference network stations and sent the modeling parameters to the GNSS users to be introduced as a priori values, with an appropriate uncertainty.

Within this context, the main issue is to take into account the influence of the Uncalibrated Phase Delays, UPD (Blewitt, 1989; Ge et al. 2008). UPDs are caused by the GNSS signals propagation through the hardware installed on either satellite or receiver. Since their values do not belong to the integer's domain and they are strongly correlated with the ambiguities, a difficulty arises in their resolution. The process of separating the UPDs from ambiguities enables the knowledge of the integer number of cycles at the moment of the first observation, that is, it accelerates AR, enabling near-instantaneous AR. It should be noted that in PPP processing without AR, UPDs are estimated grouped with ambiguities. Such a procedure leads to a longer observation time in the field. When considering the estimation of the UPDs and AR, the convergence time decreases and the positioning accuracy improves (Ge et al. 2008; Geng et al. 2010). Currently, there are three different methods for AR in PPP: the UPD Estimation Model (Ge et al. 2008), the Integer Recovery Clocks (IRC) Model (Laurichesse et al. 2008) and the Decoupled Clock Model (Collins et al. 2010); the latter is used in RTKLIB v. 2.4.2, with some mathematical modifications (Takasu and Yasuda, 2009).

Besides the UPDs influence in the convergence time necessary for ambiguities and positioning accuracy, there

is also the effect of Earth's atmosphere, which generates an advance and delay in GNSS carrier phase measurements. The advance (negative delay) occurs when the signal propagates through charged particles (electrons and free ions) in the ionosphere or Total Electron Content – TEC. The positive delay is due to the amount of hydrostatic and non-hydrostatic gases present in the neutral atmosphere, mainly in the troposphere, which contains most of these gases (Camargo, Monico and Ferreira, 2000; Teunissen and Montenbruck, 2017; Gouveia et al. 2020).

In dual-frequency receivers, the ion-free (IF) combination can be used to eliminate the first-order effects of the ionosphere, which represent approximately 99% of the total ionospheric delay (Marques, Monico and Aquino, 2011). The tropospheric delay can be estimated as an unknown term in the least-squares adjustment, mitigated using tropospheric models, or from external information. Such methodologies have different characteristics and mathematical formulations. When the tropospheric delay is not properly corrected, the remaining error may influence the AR and, consequently, the positioning and timing accuracy (Shi 2012). Thus, this research aims to assess the influence of different tropospheric correction alternatives on GPS AR for static PPP, providing directions to users when choosing a suitable tropospheric model for application in PPP-AR under Brazilian atmospheric conditions.

The tropospheric effect on PPP ambiguity has been analyzed (e.g.: Shi and Gao, 2012; Shi and Gao, 2014b; Ma et al. 2021). However, this research has some details that make it unique, such as the use of regional Brazilian NWP model; Assessment using free available (source code included) software (RTKLIB) to perform PPP-AR; Assessment of PPP-AR regarding the case of the Brazilian region. Thus, this study is representative of the experiment conditions and represents a contribution for Brazilian users as it is.

## 2. Tropospheric Delay

The neutral atmosphere can cause a propagation error of up to 30 meters for satellites at lower elevation angles, so it is one of the largest sources of systematic error in GNSS positioning (Seeber 2003; Gouveia et al. 2020). The neutral atmosphere can be divided into two components: the dry gases, the hydrostatic component, representing approximately 90% of the Zenith Total Delay (ZTD); and the water vapor, called the non-hydrostatic component, representing around 10% of the ZTD. However, its variation is much larger and can reach up to 20% in a few hours, which makes impossible its prediction (Spilker 1996; Nievinski and Santos, 2010; Gouveia et al. 2020). The hydrostatic and non-hydrostatic terms are determined separately, once they represent distinct characteristics and consequently affect GNSS signals in different ways (Spilker 1996; de Oliveira et al. 2017).

There are several ways to correct tropospheric effects, such as empirical models, ZTD estimation, and from external data, such as Numerical Weather Prediction (NWP) models and accurate troposphere files. The main disadvantage of classical empirical models such as Hopfield (1969) and Saastamoinen (1973) is that the data used are concentrated in the Northern Hemisphere and may present major differences from those in the Southern Hemisphere, which undergo sudden variations due to the tropical climate. In Brazil, in particular, there is the influence of the Amazon rainforest, which strongly affects water vapor, temperature, and pressure, over a day, according to the location (Alves et al. 2016; Fan et al. 2016).

Some researches in the literature point out the importance of estimating tropospheric gradients that consider the effects in the horizontal directions (i.e., in terms of azimuth) (Davis et al. 1993; Meindl et al. 2004; Morel et al. 2021). However, some initial experiments with the RTKLIB v.2.4.2 software demonstrated that the results were more accurate without the use of tropospheric horizontal gradients. This is the reason why they are not used in in this research. However, for future research, there is the intention to investigate this issue and consider it.

Thus, the ZTD forecasts generated by NWP models are being increasingly studied by the scientific community (Sapucci et al. 2006; Shi et al. 2015; Alves et al. 2016; Zhang et al. 2017; Gouveia et al. 2020). An NWP model contains information on weather data forecasts such as temperature, pressure, and moisture for several vertical levels. Thus, it considers more fully the regional and temporal weather variations. This information can be used to estimate the ZTD spatial distribution at the same time intervals as the numerical model generates the forecasts. In 2012, the Center for Weather Forecasting and Climate Studies (CPTEC) of the National Institute for Space Research (INPE) released a version of the regional NWP model called Eta15km (Gouveia et al. 2014), with a horizontal spatial resolution of 15 km, 3h time resolution, and 22 vertical levels.

An important issue when estimating ZTD parameters in the GNSS processing is the additional convergence time required for a proper solution. Specifically for the case of AR PPP, Shi and Gao (2014) indicate that the AR search in the PPP does not allow the convergence of the tropospheric parameter immediately. Instead, only after the ambiguity parameters are fixed to their integer values the convergence of the tropospheric parameter is accelerated. The same authors also indicate that it is common for the troposphere's convergence to require more than one hour of observation. When there is no convergence, the residual error of the tropospheric refraction degrades other unknown parameters, especially the vertical coordinate. About the ZTD Estimation strategy, both zenith hydrostatic delay (ZHD) and zenith non-hydrostatic or wet delay (ZWD) parameters are initialized with values from some model or external source.

### 3. IRC Method for PPP-AR

In the AR IRC Model (Laurichesse et al. 2008), the first-order ionospheric delay is canceled out with the IF combination, using the carrier phases  $L_1$  and  $L_2$ . The AR is performed based on three equations: the IF equation (1) and (2); and the Melbourne-Wübbena (MW) linear combination (3).

$$P_{IF} = \rho + cdt_{P_{IF}}^r - cdt_{P_{IF}}^s + T + \varepsilon_{P_{IF}} \quad (1)$$

$$L_{IF} = \rho + cdt_{P_{IF}}^r - cdt_{P_{IF}}^s + T - \lambda_{IF} N_{IF} + (b_{L_{IF}}^r - b_{P_{IF}}^r) - (b_{L_{IF}}^s - b_{P_{IF}}^s) + \varepsilon_{L_{IF}} \quad (2)$$

$$A_{MW} = -\lambda_{WL} N_{WL} + (b_{A_{MW}}^r - b_{A_{MW}}^s) + \varepsilon_{A_{MW}} \quad (3)$$

Where  $\rho$  stands for the geometric distance between receiver and satellite;  $c$  is the speed of light in vacuum;  $dt_{P_{IF}}^r$  and  $dt_{P_{IF}}^s$ , respectively, the satellite and receiver iono-free clock error;  $T$  is the tropospheric delay;  $\lambda_{IF}$  is the ionosphere-free wavelength;  $N_{IF}$  is the ionosphere-free ambiguity;  $b_{P_{IF}}^r$  and  $b_{L_{IF}}^r$  are respectively receiver code and phase hardware biases;  $b_{P_{IF}}^s$  and  $b_{L_{IF}}^s$ , respectively, satellite code and phase hardware biases;  $\varepsilon_{P_{IF}}$  and  $\varepsilon_{L_{IF}}$  are terms containing, respectively, the code and phase noise and multipath;  $b_{A_{MW}}^r$  and  $b_{A_{MW}}^s$  are the Wide-lane Receiver Bias and the Wide-lane Satellite Bias, respectively.

According to Shi and Gao (2014)  $\lambda_{IF} = \frac{2cf_0}{f_1^2 - f_2^2}$ , with the GPS carrier frequencies ( $L_1$  and  $L_2$ ):  $f_1 = 154f_0$  and  $f_2 = 120f_0$ , considering  $f_0 = 10.23\text{MHz}$ . The Wide-lane Ambiguity  $N_{WL}$ , that equates to  $N_{WL} = N_1 - N_2$ . More details on the network and user solutions for the IRC can be found in Laurichesse et al. (2008) and Shi and Gao (2014b).

## 4. Material and Methods

### 4.1 Site and period selection

To study the effect of tropospheric refraction on the positions, the same evaluation was sought in different scenarios of the neutral atmosphere. That is, in different regions of the Brazilian territory, in the summer and winter periods. For this, it was considered data from the active stations of the Brazilian Network for Continuous Monitoring of the GNSS Systems (RBMC) (IBGE, 2021). In addition, it was obtained values of the climatological variables (temperature and rainfall) from the CPTEC/INPE. Relative humidity values (%) in atmospheric layers from radiosonde data from the Department of Atmospheric Sciences of the University of Wyoming. Both data are made available free of charge to users from the institutions' websites. To choose the areas of study, this research considered locations with different climatological characteristics and used the radiosonde data to select the day with higher humidity in January and the day with less humidity in July for each RBMC station. These radiosonde data were not directly used in GNSS positioning. Some of the atmospheric data sources for the development of the research are presented in Table 1.

**Table 1:** Atmospheric data sources.

Data	Source
Radiosonde data	Made available by the University of Wyoming of the United States of America, obtained at: <a href="http://weather.uwyo.edu/upperair/sounding.html">http://weather.uwyo.edu/upperair/sounding.html</a>
CPTEC/INPE climatology data	Obtained at: <a href="http://infoclima1.cptec.inpe.br/#">http://infoclima1.cptec.inpe.br/#</a>
ZHD and ZWD data	From the NWP CPTEC/INPE model

Six RBMC stations were selected: Porto Velho (POVE) and São José da Cachoeira (SAGA), located in the northern region; Natal (RNNA), located in the Northeast region; Curitiba (UFPR) and Santa Maria (SMAR), located in the South region; and Brasília (BRAZ), in the Midwest region. Figure 1 shows the distribution of these stations. The experiment days, as well as the characteristics of the selected stations, are shown in Table 2. The radiosonde data indicated a higher humidity in the neutral atmospheric layers in the summer (Appendix 1).



Source: Google Earth (2019).

**Figure 1:** Location of the RBMC stations used in the experiments.

**Table 2:** Characteristics of Seasons and periods of experiment.

Stations	Height (m)	Köppen–Geiger Climate	Annual Average Temperature (°C)	Dates for Experiments (summer and winter)
BRAZ	1106.02	Tropical savanna (Aw)	21.1	2014-01-18 & 2014-07-03
POVE	119.59	Tropical monsoon (Am)	26.0	2014-01-19 & 2014-07-31
RNNA	45.965	Tropical savanna (Aw)	25.8	2014-01-30 & 2014-07-15
SAGA	94.886	Tropical rainforest (Af)	26.4	2014-01-02 & 2014-07-24
SMAR	113.107	Humid subtropical (Cfa)	19.3	2014-01-15 & 2014-07-22
UFPR	925.807	Oceanic (Cfb)	17.1	2014-01-04 & 2014-07-19

To reduce the impact of ionospheric effects, ionospheric scintillation periods were avoided (de Oliveira, Monico and Morel, 2020). Therefore, the experiments were performed from 12h UTC to 13h UTC. In addition, 12h UTC is one of the release times for radiosonde data and ZHD and ZWD data from the Eta15km model. This makes the data more accurate, once they are not obtained from interpolation. The data of the Eta15km model was linearly interpolated over time.

## 4.2 GNSS processing and evaluation

For the positioning processing, it was used the free software RTKLIB (Takasu, 2009), version 2.4.2. It has the option of processing PPP with AR experimentally, based on the IRC Method (Laurichesse et al. 2008). One advantage of the application of this method is that it does not use differentiated observables, as in the method of UPDs elimination proposed by Ge et al. (2008). This means that the user does not need to have observations directly from a reference network in their surroundings at the time of processing. It is only necessary to use the satellite clock correction products (.grg files), which are used in the mathematical process to preserve the integer nature of ambiguities (Laurichesse, 2011). These files are made available free of charge by the National Center for Space Studies (CNES - *Centre National D'Études Spatiales*).

Saastamoinen model and ZTD estimation alternatives are both available in RTKLIB v.2.4.2. The RTKLib version was also modified to import external data for tropospheric modeling, as the data from Eta15km.

For each RBMC station, 48 processing setups were performed, according to Figure 2 (3 tropospheric correction models, 4 observation intervals, 2 options regarding the AR, and 2 seasons – summer and winter). Processing configurations are shown in Table 3.

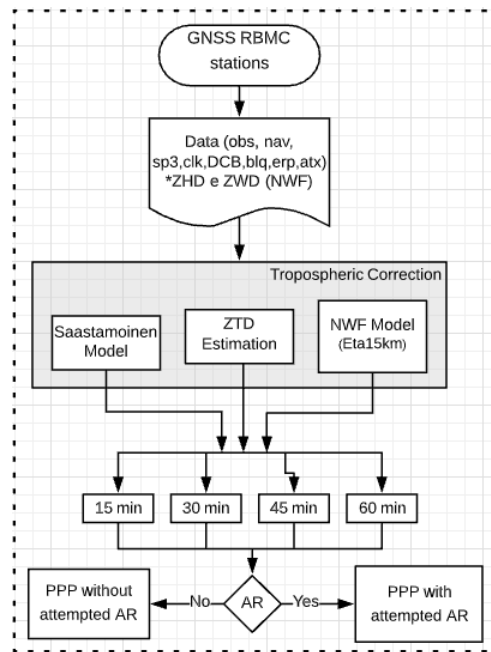


**Figure 2:** Procedures Performed in GNSS Processing.

**Table 3:** Data processing configurations.

Setting/Option	Processing configuration
Elevation mask	10°
Data sampling interval	15 seconds
Ionospheric refraction	Ion-free (L1/L2)
DCB (Differential Code Bias) C1CC1W	DCB files (CODE - Center for Orbit Determination in Europe)
Satellite's orbit and clock	Precise ephemeris files (.SP3) Crustal Dynamics Data Information System (CDDIS) of the National Aeronautics and Space Administration (NASA)
Ambiguity	IRC Model (Laurichesse et al. 2008)
Antennas phase center	NGA ANTEX file
Pole motion	Final files of Earth Rotation Parameters (.erp)
Ocean tide loading	FES2004 model
Satellite clock correction	*clk files from CNES/GRG

The RTKLIB 2.4.1 default mapping function, the Niell mapping function (Niell, 1996), was employed in this study. The processing used GPS C1C and C2W code measurements as well as L1 and L2 phase measurements. GLONASS observations were not considered, since there is no possibility in RTKLIB to attempt AR for signals from this constellation. In addition to this, the .grg files do not provide Wide Lane bias for the GLONASS constellation.

Positioning accuracy was quantified in terms of Root-Mean-Square Error (RMSE) which accounts for both bias and precision (MONICO et al. 2009). RMSEs are calculated using the discrepancies between the estimated coordinates and the official RBMC coordinates published from SIRGAS Continuously Operating Network (SIRGAS-CON), taking into account their standard-deviations. The RMSE results were obtained in the Local Geodetic System. Then, they were separated into horizontal (4) and vertical (5) components. The equation used for the determination of RMSE in each component was (MIKHAIL and ACKERMANN, 1976; MONICO et al. 2009):

$$RMSE_H = \sqrt{\Delta E^2 + \sigma_E^2 + \Delta N^2 + \sigma_N^2} \quad (4)$$

$$RMSE_U = \sqrt{\Delta U^2 + \sigma_U^2} \quad (5)$$

the term  $\Delta$  represents the difference between the estimated coordinate and the RBMC official coordinate; and  $\sigma$  is the standard deviation of the final solution, both obtained in the last adjustment epoch.

## 5. Results and Discussions

The AR did not obtain a fixed solution using the Saastamoinen model. On the other hand, both the application of the eta15km model data and the use of the ZTD Estimation provided AR convergence after certain observation periods. The times of occurrence of AR are shown in Table 4.

**Table 4:** AR convergence time using the Eta15km model and the ZTD Estimation.

Seasons	ETA15km Model		ZTD Estimation	
	Summer	Winter	Summer	Winter
BRAZ	23.5 min	28.75 min	17 min	28.25 min
UFPR	23 min	25.25 min	22 min	26.5 min
RNNA	17.25 min	34 min	17.75 min	36.5 min
POVE	24.25 min	21.75 min	16.5 min	24.75 min
SMAR	20.25 min	27.75 min	16.25 min	9.25 min
SAGA	36 min	24.5 min	13.75 min	28 min

According to Table 4, it is possible to see that for most stations, the time to reach AR was shorter in the summer than in the winter. The exceptions are POVE and SAGA stations with the ETA15km model, and the SMAR station with the ZTD Estimation. With the ZTD Estimation the AR occurred faster than with the ETA15km model in the summer. On the other hand, in winter the AR was faster with the ETA15km model. In this case the only exception is SMAR station. This may have a correlation with the suitability of tropospheric modeling in this sites locations. Probably, the ETA15km model could properly fit most of the real physical tropospheric characteristics in conditions of lower humidity, especially in the winter. On the other hand, the ZTD Estimation has shown to be the most adequate to model the delay in high humidity scenarios, especially in summer period. However, further investigations are required to draw a definitive conclusion.

Regarding the accuracy, Figures 3, 4, 5 and 6 show the behavior of the RMSE values along with the observation times for the horizontal and vertical components, without and with the AR attempt, for each of the tropospheric corrections used. In the Figures, the acronym "no-AR" indicates no AR attempt.

As presented in Figure 3, about horizontal accuracy during the summer for the no-AR experiments, the use of the Saastamoinen model provided the least accurate results when compared to the others. There was practically no change in the accuracy no-AR and with AR attempt using the Saastamoinen model, since it did not converge in any case. Such results were already expected, considering that this model was elaborated with climatic parameters that do not represent the actual conditions of the troposphere of the Brazilian territory. Additionally, due to its characteristics, the Saastamoinen model tends to model only part of the tropospheric effect, since the relative humidity of the air is fixed at 70%.

Regarding the Eta15km model and the ZTD Estimation, from 30 minutes, the RMSE values did not exceed 11 cm. The lowest value occurred in the SMAR station, the one with the lowest humidity during the summer, whose RMSE was less than 6 cm with the Eta15km model and the ZTD Estimation. However, with the AR attempt using the Eta15km model and the ZTD Estimation, there was a greater discrepancy in the RMSE results, mainly in the POVE station with the Eta15km model (approximately 37 cm). It is worth mentioning the high humidity present in the region where this station is located, being even higher than in the SAGA season during the summer, according to Appendix 1.

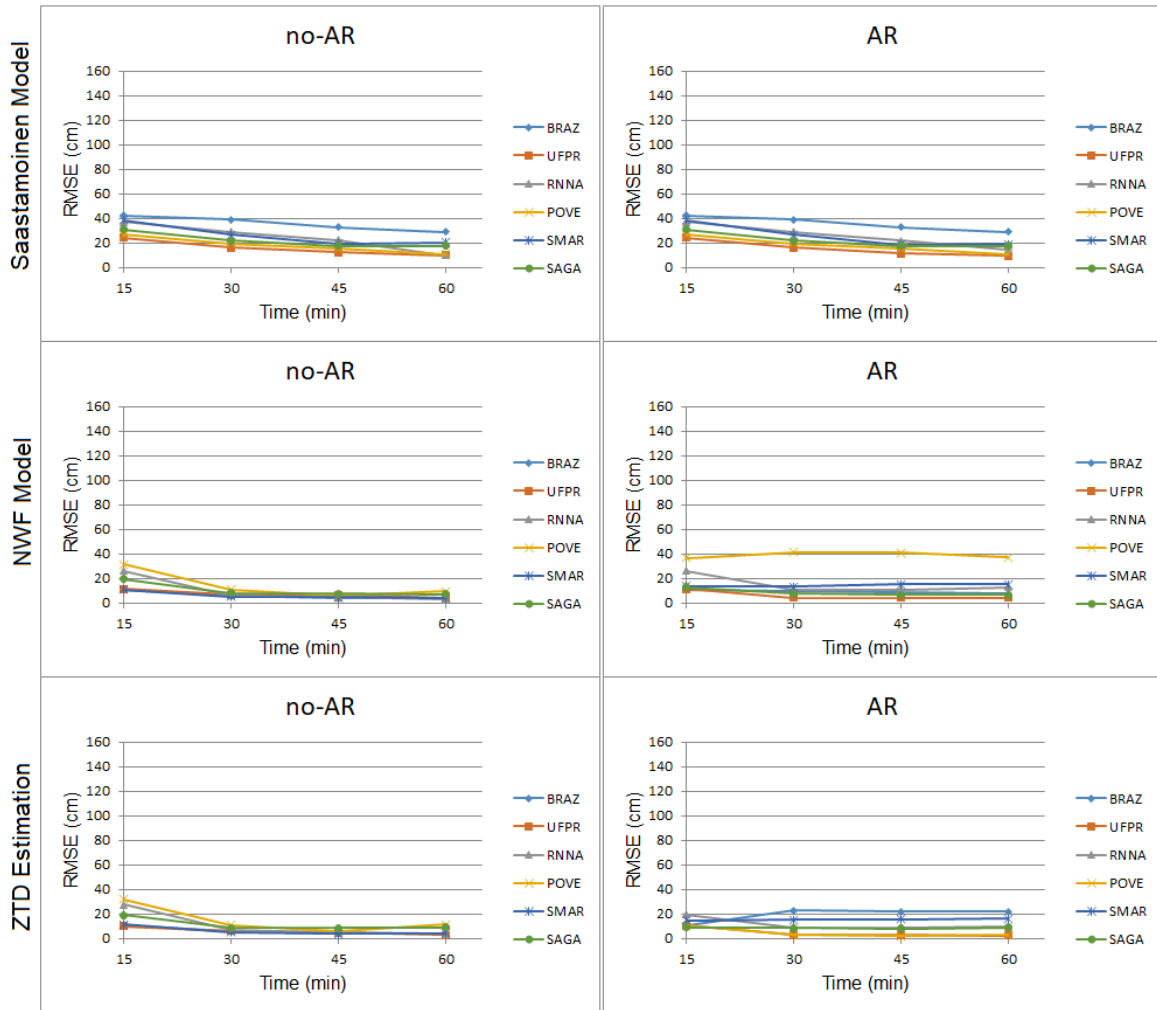


**Figure 3:** Comparison of Results of RMSE Horizontal Component (Summer).

There were oscillations between improvements and degradation of accuracy with the AR for both the Eta15km model and the ZTD Estimation. The degradation indicates possible causes of poor AR (bad fix), mainly evidenced in the accuracy of the vertical component, as shown in Figure 4.

In Figure 4, it is possible to verify that the Saastamoinen model provided less accurate results no-AR and with AR attempts. In general, RMSE values were above 40 cm. When applying data from Eta15km and using the estimation of ZTD, in the no-AR cases, the results were more consistent and accurate, with RMSE values below 20 cm after 30 minutes of observation, converging to approximately 11 cm or less with the increase of observations. Considering the AR attempt, the data from Eta15km only show improvements in accuracy at BRAZ, POVE and UFPR stations, ranging from a few millimeters to approximately 5 cm.

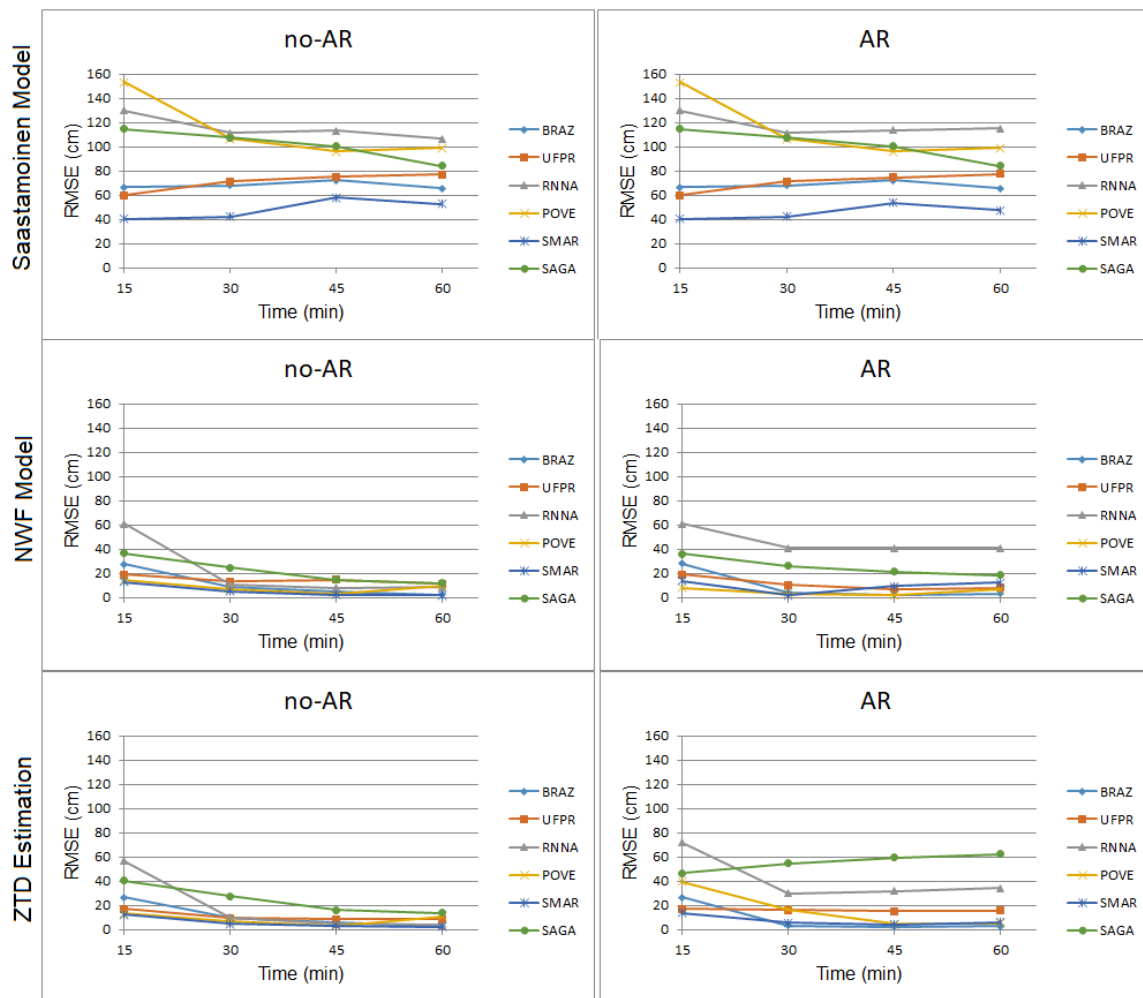


**Figure 4:** Comparison of the Results of the RMSE Vertical Component (Summer).

Particularly for RNNA and SMAR stations, results started degrading after 30 minutes of observation. This may be related to some significant change in the tropospheric layer of the region, which could not be modeled due to the temporal resolution of data from Eta15km (3 hours). In addition, the region of the SMAR station presented the highest variation of the ZWD value. The RNNA station is at the lowest altitude when compared to the other stations. Thus, there is a larger tropospheric layer over this station.

Regarding the use of the ZTD Estimation, the improvements with the AR attempt occurred at the BRAZ station after 30 minutes of observation, and in the 60 minutes of the final solution at the POVE station. These improvements ranged from 1 cm to 5 cm, being the most significant at the BRAZ station in the 30 minutes observation interval. However, significant accuracy degradation occurred with AR attempts on SAGA and RNNA stations. There was no correlation between the improvements with the ZWD component.

Cases of poor AR may be related to the fact that when one has the AR process, the results become more sensitive to the qualities of systematic error modeling. In the case of the troposphere, there is a strong dependence on a good local response in the modeling. If there is inconsistency in the model, the remaining error will be absorbed by the ambiguity parameters, which can lead to incorrect integers (bad fix).

When using data from Eta15km, the cases of bad fix may be related to the temporal and spatial resolutions of the model, which does not allow the modeling of small fluctuations of ZHD and ZWD that occur at intervals of less than three hours and distances shorter than the resolution of the 15 km grid. In the case of the use of the ZTD Estimation, the cases of a bad fix did not relate to issues of higher or lower humidity, altitude, or variation of ZWD.

Thus, these cases may be related only to the issue indicated in Shi and Gao (2014b). According to the authors, in the PPP-AR, there is a common situation where the convergence of the tropospheric parameter requires an observation time greater than one hour. Residual errors from non-convergence can be absorbed by ambiguities and can lead to poor AR.

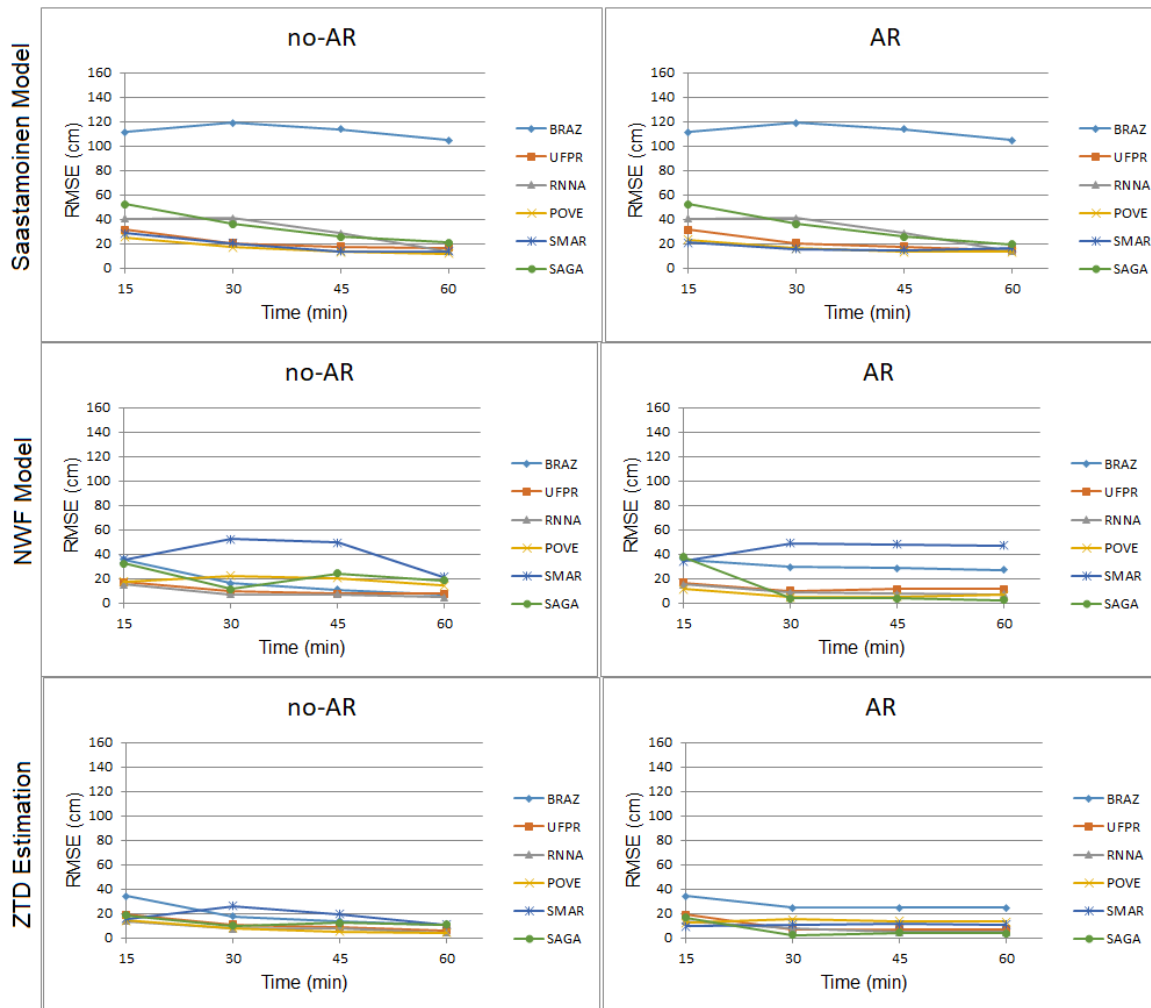


**Figure 5:** Comparison of the Results of the RMSE Horizontal Component (Winter).

For the winter, the behavior of the RMSE values for the horizontal component is shown in Figure 5. As presented, as well as in the summer, the use of the Saastamoinen model provided the least accurate results in the horizontal component. The RMSE values converged to 15 cm in the final 60-minute solution of observation, except for the BRAZ station, which presented RMSE above 100cm. Overall, the results were more accurate than the ones obtained during summer. This result is probably due to the lower amount of moisture to be modeled. Although there was no AR in any of the experiments, an improvement of 2 cm of accuracy was observed in the UFPR station with the AR attempt. In the other seasons, the results were practically the same.

Regarding the Eta15km model, except for SMAR and BRAZ, the results with AR were more accurate than in no-AR, with RMSE values below 10cm with only 30 minutes of observation. In the case of the ZTD Estimation, except for BRAZ and POVE, the RMSE values were approximated or more accurate using the AR attempt. Still in the winter, the behaviors of the RMSE values for the vertical component are shown in Figure 6. In the case of the SMAR station, it was obtained significant degradations in vertical component accuracy when using the Eta15km model, which shows probable cases of bad fix (Figure 6). This may be related to the issue of the sensitivity of the results to the quality of the tropospheric refraction modeling in the AR process, associated with the temporal and spatial resolution issues of the model.

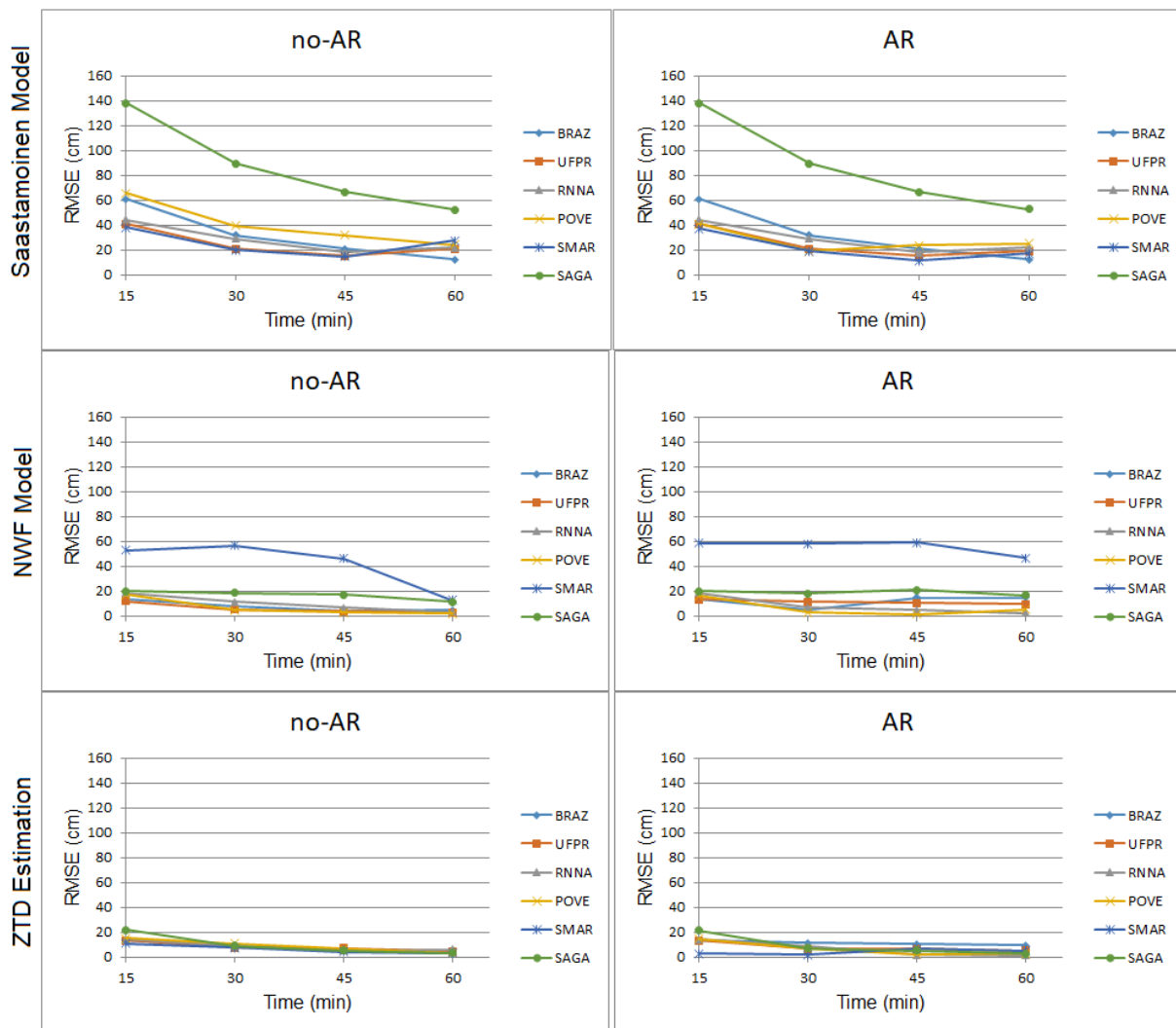


Figure 6: Comparison of the Results of the RMSE Vertical Component (Winter).

As presented in Figure 6, for the vertical component, the use of ZTD Estimation provided more accurate results than those obtained from the use of the Saastamoinen model and the Eta15km model, no-AR and with AR attempt. As expected, with the use of the Saastamoin model, it was obtained less accurate values.

## 6. Conclusions

This study evaluated the impact of different types of tropospheric correction on PPP-AR, using a method based on the ICR method (Laurichesse et al. 2008), available in the RTKLIB v. 2.4.2 software. The use of the Saastamoinen empirical model, the use of data from the Eta15km NWP model, and the use of the ZTD Estimation have been analyzed. The most significant improvements occurred in the vertical component during the winter when using the ZTD Estimation. It can also be seen that, in most experiments, during the summer, the results were less accurate than the winter's. This was expected due to the higher humidity that summer presents in relation to winter, in the tropospheric layers.

According to the results presented, it was possible to observe that considering or not AR attempt, the use of the Saastamoinen model provided the worst horizontal and vertical accuracy. Moreover, its use did not allow AR in any of the experiments. On the other hand, using 30 minutes data, the NWP model and the ZTD Estimation provided

RMSE at the centimeter level for all RBMC stations in the horizontal component no-AR. Such results agree with the studies presented in Alves et al. (2011, 2016). However, only the ZTD Estimation provided centimeter level accuracy for the no-AR vertical component. In the winter, the ZTD Estimation also provided accuracy at the centimeter level for most stations with 30 minutes of data in both, horizontal and vertical components, considering no-AR. On the other hand, the NWP model still showed accuracy at the decimeter level for most stations.

In certain experiments, AR significantly degraded the results of vertical accuracy, pointing to possible cases of bad fix, which corroborates the results obtained by Angrisano et al. (2020). This may be related to the fact that when considering AR attempts, results become more sensitive to the tropospheric modeling quality. The remaining modeling errors are absorbed by ambiguity parameters, which can lead to incorrect integers (bad fix). In our contribution, bad fix percentages were not assessed in details, since it would demand further modifications in RTKLIB source code. From experience, it is known that a bad ambiguity fixing can occur for many reasons. Typically, an indication of a bad fixed solution can be observed when an estimated position based PPP-AR present certain level of precision ( $\sim$ cm), but site coordinates differs significantly ( $\sim$ dm or even  $\sim$ m) from ground truth coordinates. In this study, we presented most of all the investigations performed and, hopefully, the impact caused by incorrect AR fix for each tropospheric model will be analyzed in future contributions. It is worth noting that, with a higher spatial and temporal resolution of the NWP model, better results can be obtained. However, based on our findings, PPP-AR method in RTKLIB must be further improved to properly provide the main AR benefits.

This research indicates that ZTD Estimation presents more accurate results on 2D positioning than the other tropospheric models assessed, for both summer and winter periods. Thus, the use of the ZTD Estimation is highly recommended PPP no-AR, once it presents more accurate results. In addition, the ZTD Estimation method has another advantage, considering that there is no need of outside information, which could require internet connection for real-time use, for example.

Finally, this contribution gives directions to improve the knowledge of PPP-AR with different tropospheric modeling alternatives, especially for the Brazilian region. Such results can be helpful to future contributions, covering more GNSS stations and a longer periods. Furthermore, it is also recommended to use a mapping function that is more suitable for the Brazilian territory, such as BMF (Gouveia et al. 2020). This mapping function is coupled with NWP model equipped with a higher spatial and temporal resolution, such as the Weather Research and Forecasting (WRF) model, currently available at CPTEC/INPE, which could better describe the Brazilian atmosphere particularities.

## ACKNOWLEDGMENTS

The authors gratefully acknowledge Tayná A. F. Gouveia, from State University of São Paulo (Unesp), for providing NWP model data. We also express our gratitude to Tomoji Takasu (RTKLIB software author), to data providers (IBGE, CNES, CDDIS/NASA), to CAPES for funding this study.

## AUTHOR'S CONTRIBUTION

All authors contribute equally.

## REFERENCES

- Alves, C. M. D., Monico, J. F. G. and Romão, V. M. C. (2011). Análise da acurácia no PPP a partir da solução de ambiguidades GPS em curtos períodos de ocupação [Analysis of PPP Accuracy from GPS Ambiguity Resolution with Short Periods of Occupation]. *Revista Brasileira de Cartografia*, 63 (5), pp.589–600.
- Alves, D. B. M. et al. (2016). Using a regional numerical weather prediction model for GNSS positioning over Brazil. *GPS Solutions*, 20 (4), pp.677–685. [Online]. DOI: 10.1007/s10291-015-0477-x.
- Angrisano, A. et al. (2020). Performance Assessment of PPP Surveys with Open Source Software Using the GNSS GPS–GLONASS–Galileo Constellations. *Applied Sciences*, v. 10, n. 16, pp. 5420. DOI: 10.3390/app10165420.
- Blewitt, G. (1989). Carrier phase ambiguity resolution for the Global Positioning System applied to geodetic baselines up to 2000 km. *Journal of Geophysical Research*, 94 (B8). [Online]. DOI: 10.1029/jb094ib08p10187.
- Camargo, P. D. O., Monico, J. F. G. and Ferreira, L. D. D. (2000). Application of ionospheric corrections in the equatorial region for L1 GPS users. *Earth, Planets and Space*, 52 (11), pp.1083–1089. [Online]. DOI: 10.1186/bf03352335.
- Choi, B.-K. et al. (2012). Precise Orbit Determination of GRACE-A Satellite with Kinematic GPS PPP. *Journal of Positioning, Navigation, and Timing*, 1 (1), pp.59–64. [Online]. DOI: 10.11003/jkgs.2012.1.1.059.
- Collins, P. et al. (2010). Undifferenced GPS ambiguity resolution using the decoupled clock model and ambiguity datum fixing. *Navigation, Journal of the Institute of Navigation*, 57 (2), pp.123–135. [Online]. DOI: 10.1002/j.2161-4296.2010.tb01772.x.
- Davis, J. L. et al. (1993). Ground-based measurement of gradients in the “wet” radio refractivity of air. *Radio Science*, v. 28, n. 6, pp. 1003-1018. DOI: 10.1029/93RS01917.
- Fan, F. M. et al. (2016). Flood forecasting on the Tocantins River using ensemble rainfall forecasts and real-time satellite rainfall estimates. *Journal of Flood Risk Management*, 9 (3), pp.278–288. [Online]. DOI: 10.1111/jfr3.12177.
- Ge, M. et al. (2008). Resolution of GPS carrier-phase ambiguities in Precise Point Positioning (PPP) with daily observations. *Journal of Geodesy*, 82 (7), pp.389–399. [Online]. DOI: 10.1007/s00190-007-0187-4.
- Geng, J. et al. (2010). Integer ambiguity resolution in precise point positioning: Method comparison. *Journal of Geodesy*, 84 (9), pp.569–581. [Online]. DOI: 10.1007/s00190-010-0399-x.
- Geng, J. and Shi, C. (2017). Rapid initialization of real-time PPP by resolving undifferenced GPS and GLONASS ambiguities simultaneously. *Journal of Geodesy*, 91 (4), pp.361–374. [Online]. DOI: 10.1007/s00190-016-0969-7.
- Gouveia, T. A. F. et al. (2014). Avaliação robusta da modelagem neutrosférica sobre o território brasileiro baseada em modelos de previsão numérica de tempo da América do Sul [Robust evaluation of neutrospheric modeling over brasilian territory based on numerical weather prediction models of South American]. *Boletim de Ciências Geodésicas*, v. 20, p. 481-503. DOI: 10.1590/S1982-21702014000200028.
- Gouveia et al. (2020), 50 years of synergy between space geodesy and meteorology: from a GNSS positioning error to precipitation nowcasting applications. *Revista Brasileira de Cartografia*. v. 72, 50th Anniversary Special Issue, 2020. DOI:10.14393/rbcv72nespecial50anos-56767.
- Hopfield, H. S. (1969). Two-quartic tropospheric refractivity profile for correcting satellite data. *Journal of Geophysical Research*. 74(18), 4487-4499. DOI 10.1029/JC074i018p04487.
- Instituto Brasileiro de Geografia e Estatística - IBGE. (2021). Solução Multianual das Estações da Rede Brasileira de Monitoramento Contínuo dos Sistemas GNSS no Período de 2000 a 2019 [Multiannual Solution for the Brazilian Network for Continuous Monitoring of the GNSS Systems from 2000 to 2019]. Rio de Janeiro. *IBGE*, 49, pp. 117. Available at: <<https://biblioteca.ibge.gov.br/visualizacao/livros/liv101895.pdf>>.
- Kouba, J. and Héroux, P. (2001). Precise Point Positioning Using IGS Orbit and Clock Products. *GPS Solutions*. 5(2), 12-28. DOI 10.1007/PL00012883.

- Laurichesse, D. (2011). The CNES Real-time PPP with undifferenced integer ambiguity resolution demonstrator. *24th International Technical Meeting of the Satellite Division of the Institute of Navigation 2011, ION GNSS 2011*, 1, pp.654–662.
- Laurichesse, D. et al. (2008). Real Time Zero-difference Ambiguities Fixing and Absolute RTK. *Proceedings of the 2008 National Technical Meeting of The Institute of Navigation*, San Diego, CA, January, pp. 747-755.
- Li, Y., Li, B. and Gao, Y. (2015). Improved PPP ambiguity resolution considering the stochastic characteristics of atmospheric corrections from regional networks. *Sensors (Switzerland)*, 15 (12), pp.29893–29909. [Online]. DOI: 10.3390/s151229772.
- Lima, C. M. D. A., Monico, J. F. G., Marques, H. A. (2016). PPP Com Solução Inteira das Ambiguidades da Fase da Onda Portadora: Fundamentos Envolvidos e Análise de Acurácia [PPP with Integer Resolution of Carrier Phase Ambiguity: Fundamentals Involved and Accuracy Assessment]. *Revista Brasileira de Cartografia*, n. 68/5, pp. 1063-1077. Available at: <<https://seer.ufu.br/index.php/revistabrasileiracartografia/article/download/44435/23510>>.
- Ma, H. et al. (2021). Influence of the inhomogeneous troposphere on GNSS positioning and integer ambiguity resolution. *Advances in Space Research*, v. 67, n. 6, p. 1914-1928. DOI: 10.1016/j.asr.2020.12.043.
- Marques, H. A., Monico, J. F. G. and Aquino, M. (2011). RINEX\_HO: Second- and third-order ionospheric corrections for RINEX observation files. *GPS Solutions*, 15 (3), pp.305–314. [Online]. DOI: 10.1007/s10291-011-0220-1.
- Meindl, m.; Schaer, s.; Hugentobler, u.; Beutler, G. (2004). Tropospheric gradient estimation at CODE: Results from global solutions. *Journal of the Meteorological Society of Japan*. Ser. II, v. 82, n. 1B, pp. 331-338. DOI: 10.2151/jmsj.2004.331.
- Mikhail, E. M., and Ackermann, F. (1976). Observations and Least Squares University Press of America. *Lanham, MD*.
- Monico, J.F.G. et al. (2009). Acurácia e precisão: revisão dos conceitos de forma acurada [Accuracy and Precision: reviewing the concepts by means of an accurate procedure]. *Boletim de Ciências Geodésicas*, ISSN 1982-2170. Available at: <<https://revistas.ufpr.br/bcg/article/view/15513>>.
- Morel, I.; Moudni, o.; Durand, F.; et al. (2021). On the relation between GPS tropospheric gradients and the local topography. *Advances in Space Research*, v. 68, n. 4, p. 1676–1689. DOI: 10.1016/j.asr.2021.04.008.
- Niell, A. E. (1996). Global mapping functions for the atmosphere delay at radio wavelengths. *Journal of Geophysical Research B: Solid Earth*, 101 (2), pp.3227–3246. [Online]. DOI: 10.1029/95jb03048.
- Nievinski, F. G. and Santos, M. C. (2010). Ray-tracing options to mitigate the neutral atmosphere delay in GPS. *Geomatica*, 64 (2), pp.191–207.
- de Oliveira, P. S. et al. (2017). Modeling tropospheric wet delays with dense and sparse network configurations for PPP-RTK. *GPS Solutions*, 21 (1), pp.237–250. [Online]. DOI: 10.1007/s10291-016-0518-0.
- de Oliveira, P. S., Monico, J. F. G. and Morel, L. (2020). Mitigation of receiver biases in ionospheric observables from PPP with ambiguity resolution. *Advances in Space Research*, 65 (8), pp.1941–1950. [Online]. DOI: 10.1016/j.asr.2020.01.037.
- Pan, L. et al. (2021). Performance assessment of real-time multi-GNSS integrated PPP with uncombined and ionospheric-free combined observables. *Advances in Space Research*, 67 (1), pp.234–252. [Online]. DOI: 10.1016/j.asr.2020.09.029.
- Perez, J. A. S., Monico, J. F. G. and Chaves, J. C. (2003). Velocity Field Estimation Using GPS Precise Point Positioning: The South American Plate Case. *Journal of Global Positioning Systems*, 2 (2), pp.90–99. [Online]. DOI: 10.5081/jgps.2.2.90.
- RTKLIB. (2015). Manual RTKLIB, v. 2.4.2. Available at: <[http://www.rtklib.com/prog/manual\\_2.4.2.pdf](http://www.rtklib.com/prog/manual_2.4.2.pdf)>. [accessed 30 June 2019].
- Saastamoinen, J. (1973). Contributions to the theory of atmospheric refraction. *Bulletin Géodésique*. 105(1), 279-298. DOI 10.1007/BF02522083.

dos Santos, A. F. et al. (2017). Parallelism error in peanut sowing operation with auto-steer guidance. *Revista Brasileira de Engenharia Agrícola e Ambiental*, 21 (10), pp.731–736. [Online]. DOI: 10.1590/1807-1929/agriambi.v21n10p731-736.

Sapucci, L. F. et al. (2006). Previsões do atraso zenital troposférico para a América do Sul: variabilidade sazonal e avaliação da qualidade [Predictions of Tropospheric Zenithal Delay for South America: Seasonal Variability and Quality Evaluation]. *Revista Brasileira de Cartografia*, (1808–0936), pp.279–292.

Seeber, G. (2003). *Satellite Geodesy: Foundations, Methods, and Applications*. Berlin, New York: Walter de Gruyter.

Shi, J. (2012). *Precise Point Positioning Integer Ambiguity Resolution with Decoupled Clocks*. (PhD thesis, University of Calgary).

Shi, J. and Gao, Y. (2012). Improvement of PPP-inferred tropospheric estimates by integer ambiguity resolution. *Advances in Space Research*, v. 50, n. 10, p. 1374-1382. DOI: 10.1016/j.asr.2012.06.036.

Shi, J. et al. (2015). Real-Time GPS precise point positioning-based precipitable water vapor estimation for rainfall monitoring and forecasting. *IEEE Transactions on Geoscience and Remote Sensing*, 53 (6), pp.3452–3459. [Online]. DOI: 10.1109/TGRS.2014.2377041.

Shi, J. and Gao, Y. (2014a). A comparison of three PPP integer ambiguity resolution methods. *GPS Solutions*, 18 (4), pp.519–528. [Online]. DOI: 10.1007/s10291-013-0348-2.

Shi, J. and Gao, Y. (2014b). A troposphere constraint method to improve PPP ambiguity-resolved height solution. *Journal of Navigation*, 67 (2), pp.249–262. [Online]. DOI: 10.1017/S0373463313000647.

Spilker Jr J. J. (1996). Tropospheric Effects on GPS. *Parkinson BW & Spilker Jr JJ (Ed.)*. Global Positioning System: Theory and Applications. American Institute of Aeronautics and Astronautics. p. 517-546.

Takasu, T. and Yasuda, A. (2009). Development of the low-cost RTK-GPS receiver with an open source program package RTKLIB. *International Symposium on GPS/GNSS*, pp.4–6.

Teunissen, P. J. G. and Khodabandeh, A. (2015). Review and principles of PPP-RTK methods. *Journal of Geodesy*, 89 (3), pp.217–240. [Online]. DOI: 10.1007/s00190-014-0771-3.

Teunissen, P. J. G. and Montenbruck, O. (2017). Springer Handbook of Global Navigation Satellite Systems. *Springer Handbooks*.

Teunissen, P. J. G., Odijk, D. and Zhang, B. (2010). PPP-RTK: Results of CORS network-based PPP with integer ambiguity resolution. *Journal of Aeronautics, Astronautics and Aviation*, 42 (4), pp.223–230.

Yoshioka, T. and Murata, M. (2009). An Assessment of GPS-based precise point positioning of the low earth-orbiting satellite CHAMP, *ICCAS-SICE*, Fukuoka, pp. 4722-4728.

Zhang, H. et al. (2017). GPS PPP-derived precipitable water vapor retrieval based on Tm/Ps from multiple sources of meteorological data sets in China. *Journal of Geophysical Research*, 122 (8), pp.4165–4183. [Online]. DOI: 10.1002/2016JD026000.

Zheng, K. et al. (2019). Mitigation of unmodeled error to improve the accuracy of multi-GNSS PPP for crustal deformation monitoring. *Remote Sensing*, 11 (19). [Online]. DOI: 10.3390/rs11192232.

Zumberge, J. F. et al. (1997). Precise point positioning for the efficient and robust analysis of GPS data from large networks. *Journal of Geophysical Research: Solid Earth*, 102 (B3), pp.5005–5017. [Online]. DOI: 10.1029/96jb03860.

# Appendix 1

